Journal of Zhejiang University SCIENCE A
ISSN 1009-3095
http://www.zju.edu.cn/jzus
E-mail: jzus@zju.edu.cn

Advanced aerostatic analysis of long-span suspension bridges*

ZHANG Xin-jun (张新军)

(*School of Civil Engineering and Architecture, Zhejiang University of Technology, Hangzhou 310014, China*)

E-mail: xjzhang@zjut.edu.cn

Received Mar. 8, 2005; revision accepted Aug. 10, 2005

Abstract: As the span length of suspension bridges increases, the diameter of cables and thus the wind load acting on them, the nonlinear wind-structure interaction and the wind speed spatial non-uniformity all increase consequently, which may have unnegligible influence on the aerostatic behavior of long-span suspension bridges. In this work, a method of advanced aerostatic analysis is presented firstly by considering the geometric nonlinearity, the nonlinear wind-structures and wind speed spatial non-uniformity. By taking the Runyang Bridge over the Yangtze River as example, effects of the nonlinear wind-structure interaction, wind speed spatial non-uniformity, and the cable's wind load on the aerostatic behavior of the bridge are investigated analytically. The results showed that these factors all have important influence on the aerostatic behavior, and should be considered in the aerostatic analysis of long and particularly super long-span suspension bridges.

Key words: Long-span suspension bridge, Aerostatic analysis, Nonlinear wind-structure interaction, Wind speed spatial non-uniformity, Cable's wind load

doi:10.1631/jzus.2006.A0424 **Document code:** A **CLC number:** U448.25

INTRODUCTION

Two examples of the great progress achieved in recent decades in the design and construction of long-span suspension bridges are the Akashi Kaikyo Bridge (1990 m) in Japan and the Great Belt Bridge (1624 m) in Denmark. Into the 21st century, longer suspension bridges are being planned, such as the Messina strait bridge in Italy (3300 m), and the Gibraltar bridge between Spain and Morocco (5000 m) (Astiz, 1998), etc. In China, five large strait crossing projects have been planned. These strait crossing projects will consist of some large suspension bridges with span lengths of 2000~3000 m (Xiang and Chen, 1998). Many of these bridges are built in straits frequently subjected to violent typhoon or hurricane. The rapid increase in span length combined with the trend to more shallow or slender stiffening girders in suspension bridges has raised concern on their behaviors under wind action, with wind resistance being an important factor controlling their design and construction.

The aerostatic behavior of long-span suspension bridges was comprehensively investigated by Boonyapinyo *et al*.(1994), Cheng *et al*.(2002), Xiao and Chen (2004). They developed a finite element method to predict the critical wind speed on the nonlinear lateral-torsional buckling instability of long-span suspension bridges, but the influence of some factors such as the nonlinear wind-structure interaction, the cable's wind load and wind speed spatial non-uniformity on the aerostatic behavior has not been clearly clarified. With increase of bridge span, structural flexibility, the tower's height and the cable's diameter increase simultaneously, which will further enhance the above effects.

How these factors affect the aerostatic behavior of long-span suspension bridges is becoming a more and more serious problem, which must be further investigated. This work is aimed at investigating the roles of these factors in the aerostatic behavior of long-span suspension bridges.

* Project (No. 502118) supported by the Natural Science Foundation of Zhejiang Province, China

MODEL OF THE AEROSTATIC LOAD

Spatial distribution of wind speed

Generally, wind speed changes in space, and can be expressed as (Xie and Xiang, 1985):

$$U=\mu U_0,\ \mu=\left[1-\left(\frac{L-2z+e(L_1-L)}{L_1}\right)^2\right]\left(\frac{y}{10}\right)^{\alpha}, \quad (1)$$

where U_0 is the basic wind speed at the height of 10 m from the ground at the bridge site; μ is wind speed spatial distribution coefficient; L is the total length of bridge spans; L_1 is the width of wind distribution; e is the coefficient of wind speed distributing non-symmetrically, $0\le e\le 1$. When e is equal to 0, wind speed distributes symmetrically with midspan; α is the exponential coefficient of wind profile, which is dependent on the roughness of the ground; y is the height from the ground.

Nonlinear aerostatic loads

Consider a section of bridge deck in a smooth flow, as shown in Fig.1. Assuming that under the effect of the mean wind velocity U with angle of incidence θ_0, the torsional displacement of the deck is θ. Then the effective wind angle of attack is $\alpha_e=\theta_0+\theta$. As the spatial non-uniformity of wind speed is considered, three components of aerostatic loads, named as drag force, lift force and pitch moment, acting on per unit length of the deck can be expressed as

$$F_z=\rho\mu^2U_0^2DC_z(\alpha_e)/2,\ F_y=\rho\mu^2U_0^2BC_y(\alpha_e)/2,$$
$$M_x=\rho\mu^2U_0^2B^2C_M(\alpha_e)/2, \quad (2)$$

where ρ is the air density; D is the deck's vertical projected area; B is the deck's width; $C_z(\alpha_e)$, $C_y(\alpha_e)$, $C_M(\alpha_e)$ are the aerostatic coefficients obtained from the section model test in wind tunnel.

For cables and hangers, only the drag component is considered, and can be expressed as

$$F_z=\rho\mu^2U_0^2DC_D/2, \quad (3)$$

where D is the diameter of cables and hangers, C_D is the drag coefficient, which is equal to 0.7 (Xiang *et al*., 1996).

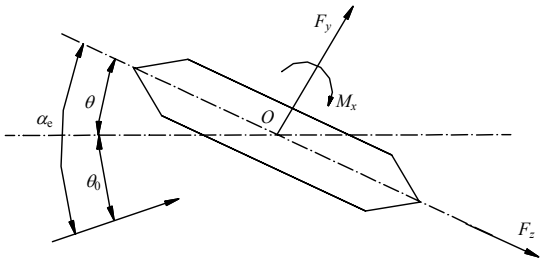

Fig.1 The aerostatic loads acting on the deck

SOLUTION PROCEDURE

The aerostatic analysis is aimed to predict the equilibrium position. Under a certain wind speed, the static equilibrium position must be solved by the iteration approach because of the non-linearity of both the structure and the displacement-dependent aerostatic loads. The iteration equation can be expressed as:

$$[\boldsymbol{K}(\boldsymbol{u})]\{\boldsymbol{u}\}=\boldsymbol{P}[F_y(\alpha_e),F_z(\alpha_e),M(\alpha_e)], \quad (4)$$

where $[\boldsymbol{K}(\boldsymbol{u})]$ is the structural stiffness matrix including linear-elastic stiffness matrix and geometrical matrix; $\{\boldsymbol{u}\}$ is the nodal displacement vector; $\boldsymbol{P}[F_y(\alpha_e),F_z(\alpha_e),M(\alpha_e)]$ is the total aerostatic load vector.

To solve the nonlinear Eq.(4), a two-iteration solution scheme is used. In the inner cycle of iteration, geometric nonlinear analysis of structure under incremental aerostatic loads is conducted using the incremental Newton-Raphson iteration method. Nonlinear analysis under incremental wind load, induced by the torsional deformation of the deck that in turn increases wind angles of attack, is performed in the outer cycle of iteration. The procedure can be summarized as follows: (1) Input the finite element model of the bridge and its aerostatic coefficients; (2) Compute the wind speed spatial distribution coefficients for each element of the bridge; (3) Perform structural nonlinear aerostatic analysis under the given wind speed U_0 to get the aerostatic equilibrium position.

The computing flow can be described as follows:

(1) Calculate the aerostatic load $\{F_0\}$ under the initial wind attack angles, and let $\{F_2\}=\{F_0\}$, $\{F_1\}=\{0\}$;

(2) Calculate incremental aerostatic load $\{\Delta F\}=\{F_2\}-\{F_1\}$, and let $\{F_1\}=\{F_2\}$;

(3) Conduct structural geometric nonlinear analysis under incremental aerostatic load to obtain the deformed position of the bridge;

(4) Determine the deck's effective wind attack angle, and recalculate the aerostatic load $\{F_2\}$;

(5) Check if the Euclidean norm of the aerostatic coefficients is less than the prescribed tolerance. The Euclidean norm is expressed as:

$$\left\{\frac{\sum_{1}^{N_a}[C_K(\alpha_j)-C_K(\alpha_{j-1})]^2}{\sum_{1}^{N_a}[C_K(\alpha_{j-1})]^2}\right\}^{1/2} \le \varepsilon_K \quad (K=y,z,M), \quad (5)$$

where ε_K is the prescribed tolerance; N_a is the total number of nodes subjected to wind action.

If satisfied, the computation is finished. Otherwise repeat Steps (2)~(4) until Eq.(5) is satisfied.

Based on the above solution procedure, a computer program BSNAA was developed for the aerostatic analysis of bridge structures (Zhang *et al*., 2002).

DESCRIPTION OF THE EXAMPLE BRIDGE

The Runyang Bridge over the Yangtze River is the longest suspension bridge in China, and has a 1490 m main span and two 470 m side spans, as shown in Fig.2. The cable's sag to span ratio is 1/10, and the spacing of cables is 34.3 m. The deck is a 3.0 m high and 35.9 m wide steel streamlined box girder. The towers are door-shaped with about 209 m high. In the following analysis, a 3D finite element model of the bridge is established, in which the deck and towers are modeled by 3D beam elements, and the hangers and cables are modeled by 3D bar elements, and rigid beams are provided to model the connections between the deck and the hangers. The connections between bridge components and the supports of the bridge are also properly modeled.

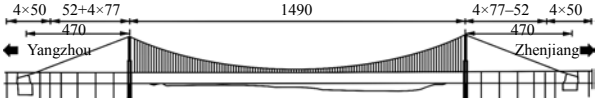

Fig.2 General configuration of Runyang Bridge (m)

AEROSTATIC ANALYSIS

In the following sections, under the initial wind attack angle of 0°, influences of the aforementioned factors on the aerostatic behavior of the bridge were investigated analytically by BSNAA. The deck's aerostatic coefficients are experimental determined results of the sectional model test in wind tunnel (Chen and Song, 2000), and the exponential coefficient of wind profile α is taken as 0.16 (Xiang *et al*., 1996).

Nonlinear wind-structure interaction

Long and super long-span suspension bridges deform significantly under static wind action due to their great flexibility. The large deformation, on the one hand, affects structural stiffness; on the other hand, changes the wind attack angle between the wind flow and the deck, and therefore leads to the variation of the aerostatic loads that are the function of the effective wind attack angle. It is called as the nonlinear wind-structure interaction herein.

Linear and nonlinear aerostatic analyses were conducted on the bridge with increase of wind speed. In the linear analysis, only the variation of wind speed was considered, while in the nonlinear analysis, both the variation of wind speed and the nonlinear wind-structure interaction were considered. The evolutions of the displacements of the deck at midspan with wind speed are plotted in Fig.3.

Fig.3 shows that the vertical and torsional displacements obtained from nonlinear analyses are both greater than those from linear analyses, and that the difference increases rapidly with increase of wind speed. Therefore, the nonlinear wind-structure interaction has significant influence on the vertical and torsional displacements. However, the lateral displacements under the two cases are identical, and basically not affected by the nonlinear wind-structure interaction. Therefore, the nonlinear wind-structure interaction should be considered in the aerostatic analysis of long-span suspension bridges.

Cable's wind load

As the bridge span increases, the cable's diameter and its vertical projected area increase, which results in the increase of wind load acting on the cable. In order to investigate how the cable's wind load aff-

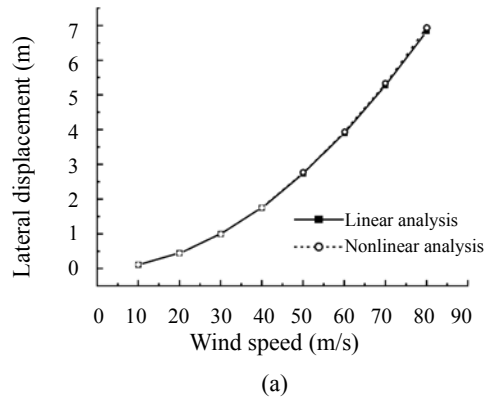

Fig.3 Influence of nonlinear wind-structure interaction on the displacements of the deck at midspan
(a) Lateral displacement; (b) Vertical displacement; (c) Torsional angle

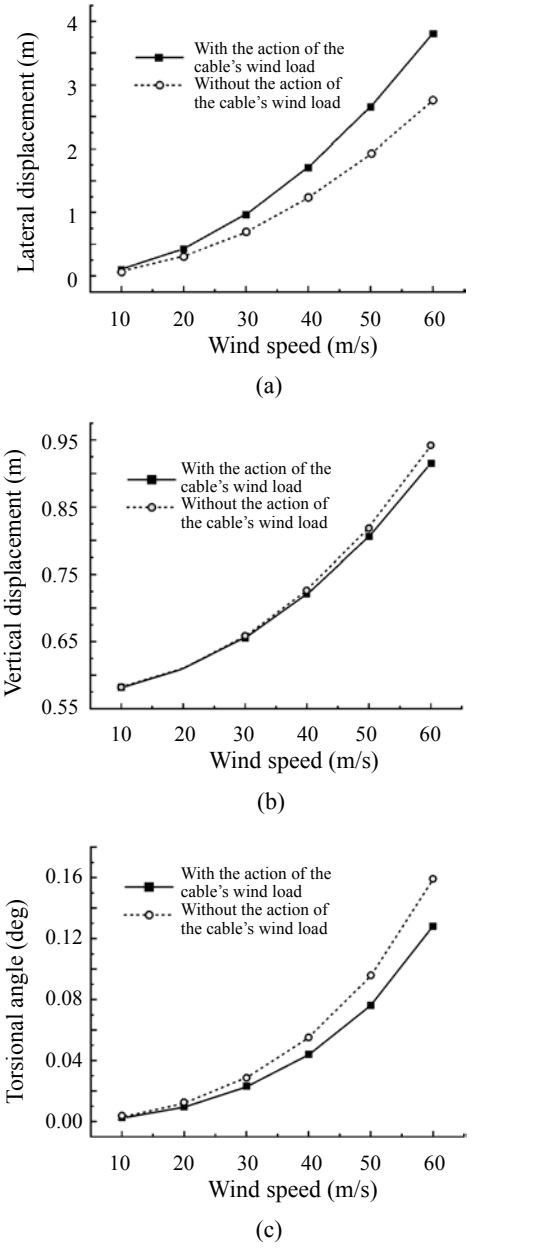

Fig.4 Influence of wind load acting on the cables on the displacements of the deck at midspan
(a) Lateral displacement; (b) Vertical displacement; (c) Torsional angle

ects the aerostatic behavior of the bridge, cases with and without the action of the cable's wind load were analyzed, and evolutions of the displacements of the deck at midspan with wind speed are plotted in Fig.4.

As seen in Fig.4, the lateral and torsional displacements are greatly affected by the cable's wind load, whereas for the vertical displacement, the influence is little. For the bridge, the diameter of a single cable is 0.7765 m, and the lateral wind load acting on a single cable is approximately 0.24 that on the deck, and therefore the lateral displacement decreases as the action of the cable's wind load is neglected. As lift load is not considered for the two cases, the vertical displacements are almost identical. Without the action of the cable's wind load, the lateral displacements of the deck are greater than those of the cables,

and greater torsional angles are achieved for the deck. When the cable's wind load is considered, the difference in the lateral displacements between the deck and cables decreases, and the torsional angles of the deck therefore decrease. Therefore, the cable's wind load must be considered in the aerostatic analysis of long-span suspension bridges.

Spatial non-uniformity of wind speed

In the previous analysis, the wind speeds at different locations were assumed to be the same. In fact, for long and particularly super long-span suspension bridges, the towers are generally very high, and the wind speeds on the cables and hangers are obviously greater than those on the deck, and therefore the wind speed becomes non-uniform in space.

Under wind speed of 60 m/s, cases with different wind distribution were analyzed. The variations of the lateral and vertical displacements, the torsional angle and the wind speed spatial distribution coefficient along the bridge axis are plotted in Fig.5 and Fig.6.

Fig.5 shows that with decrease of wind distribution width, the lateral and vertical displacement and the torsional angle are all less than those in the case of wind speed distributing uniformly. The reason is that the wind speed spatial distribution coefficient and therefore the aerostatic loads acting on the bridge are reduced. However, the effect of wind speed spatial non-uniformity on the aerostatic behavior is gradually weakened as the wind distribution width increases.

Under the same wind distribution width as shown in Fig.6, structural displacements decrease greatly as the wind speed distributes non-symmetrically. The fact can be also attributed to that the wind speed spatial distribution coefficient and thus the aerostatic loads acting on the bridge are remarkably reduced in this case. Therefore, the effect should be considered exactly in the aerostatic analysis.

CONCLUSION

In this work, by taking Runyang Bridge over the Yangtze River as example, effects of nonlinear wind-

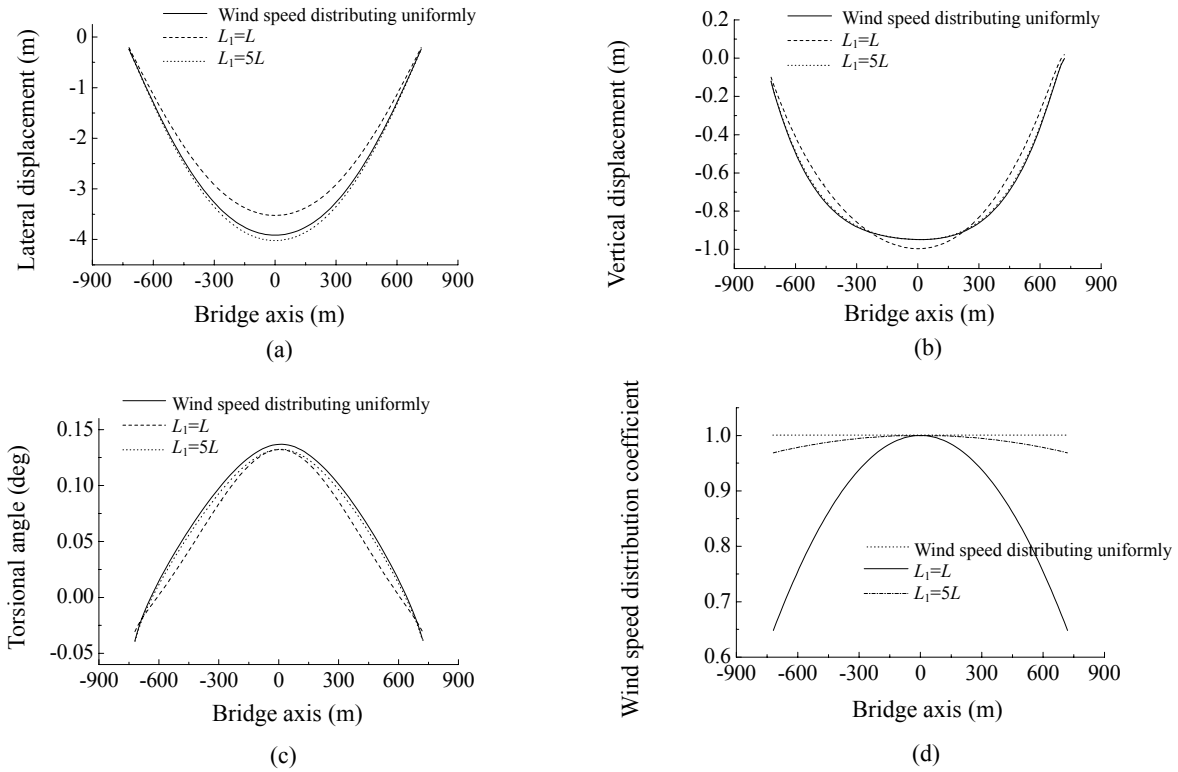

Fig.5 The displacements and wind speed spatial distribution coefficient varying along the bridge axis in the case of wind speed distributing symmetrically

(a) Lateral displacement; (b) Vertical displacement; (c) Torsional angle; (d) Wind speed distribution coefficient

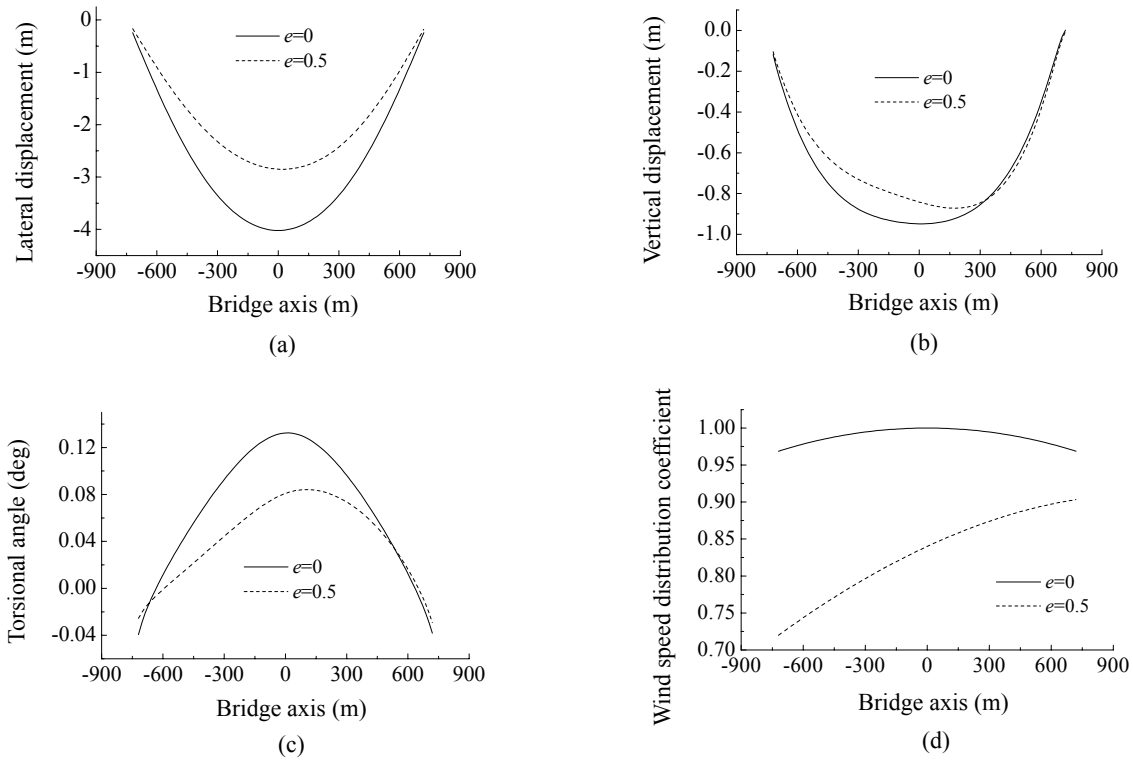

Fig.6 The displacements and wind speed distribution coefficient variation along the bridge axis under the same wind distribution width

(a) Lateral displacement; (b) Vertical displacement; (c) Torsional angle; (d) Wind speed distribution coefficient

structure interaction, wind speed spatial non-uniformity, and the cable's wind load on the aerostatic behavior of the bridge are investigated analytically by the computer program BSNAA. It is concluded that nonlinear wind-structure interaction, wind speed spatial non-uniformity, and the cable's wind load all have important influence on the aerostatic behavior of long-span suspension bridges, and should be considered in the aerostatic analysis of long and especially super long-span suspension bridges.

References

Astiz, M.A., 1998. Flutter stability of very long suspension bridges. *Journal of Bridge Engineering, ASCE*, **3**(3):132-139. [doi:10.1061/(ASCE)1084-0702(1998)3:3(132)]

Boonyapinyo, V., Yamada, H., Miyata, T., 1994. Wind-induced nonlinear lateral-torsional buckling of cable-stayed bridges. *J. Struct. Engrg., ASCE*, **120**(2):486-506.

Chen, A.R., Song, J.Z., 2000. Research on the wind resistance of Runyang Bridge over the Yangtze River. The Key Laboratory for Disaster Reduction in Civil Engineering, Tongji University (in Chinese).

Cheng, J., Jiang, J.J., Xiao, R.C., Xiang, H.F., 2002. Nonlinear aerostatic stability analysis of Jiang Yin suspension bridge. *Engineering Structures*, **24**(6):773-781. [doi:10.1016/S0141-0296(02)00006-8]

Xiang, H.F., Chen, A.R., 1998. 21st Century Long-span Bridges in China. *In*: Larsen, A., Esdah, S.(Eds.), Bridge Aerodymics. Balkema, Rotterdam.

Xiang, H.F., Lin, Z.X., Bao, W.G., Chen, A.R., Gu, M.(Eds.), 1996. Wind-resistant Design Guidebook for Highway Bridges. People's Communication Press, Beijing, China (in Chinese).

Xiao, R.C., Chen, J., 2004. Advanced aerostatic stability analysis of suspension bridges. *Wind and Structures*, **7**(1):55-70.

Xie, Q.M., Xiang, H.F., 1985. Three flutter analysis for bridges by state-space approach. *Journal of Tongji University*, **3**:1-13.

Zhang, X.J., Sun, B.N., Xiang, H.F., 2002. Nonlinear aerostatic and aerodynamic analysis of long-span suspension bridges considering wind-structure interactions. *Journal of Wind Engineering and Industrial Aerodynamics*, **90**(9):1065-1080. [doi:10.1016/S0167-6105(02)00251-9]